*Proc. Natl. Acad. Sci. USA*
Vol. 82, pp. 8629–8633, December 1985
Immunology

# Isolation and biochemical and functional characterization of perforin 1 from cytolytic T-cell granules

(T lymphocytes/cell-mediated cytolysis/polymerization/transmembrane channels/patch-clamp)

ECKHARD R. PODACK*, JOHN DING-E YOUNG†, AND ZANVIL A. COHN†

*Department of Microbiology and Immunology, New York Medical College, Valhalla, NY 10595; and †Laboratory of Cellular Physiology and Immunology, The Rockefeller University, New York, NY 10021

*Contributed by Zanvil A. Cohn, August 14, 1985*

**ABSTRACT** **The $Ca^{2+}$-dependent cytolytic activity of isolated T-lymphocyte granules was purified to apparent homogeneity by high-salt extraction, gel filtration, and ion-exchange chromatography. The lytic activity resided in a 72- to 75-kDa protein of cytolytic granules. Incubation of the isolated protein with erythrocytes in the presence of $Ca^{2+}$ ions resulted in hemolysis and the formation of membrane lesions of 160 Å in diameter, corresponding in size and morphology to membrane lesions formed on target cells by cloned, intact natural killer (NK) and cytolytic T lymphocytes. Hence, the 75-kDa granule protein is identified as monomeric perforin 1 (P1), postulated previously from the analysis of membrane lesions formed during NK and T-cell-mediated cytolysis. P1-mediated hemolysis is $Ca^{2+}$-dependent and is inhibited by $Zn^{2+}$ ions. Lysis is accompanied by the polymerization of P1 to membrane-associated tubular complexes (poly-P1) that form large transmembrane pores. P1 causes a rapid membrane depolarization of J774 cells in the presence of $Ca^{2+}$. Purified P1 also induces transmembrane monovalent and divalent ion flow across lipid vesicles only in the presence of $Ca^{2+}$. Whole-cell patch-clamp recordings of S49 lymphoma cells show a P1-dependent inward membrane current flow in the presence but not in the absence of $Ca^{2+}$. The current increase can be dissected as a summation of discrete current events, indicative of formation of functional channels by polymerization of P1.**

Target cell lysis, mediated by natural killer (NK) and cytotoxic T lymphocytes (CTL), is partially caused by the assembly of tubular transmembrane complexes on target membranes, designated polyperforin 1 (poly-P1) and 2 (poly-P2) (1–6). It has been postulated that the monomeric precursors of polyperforins are contained in the cytoplasmic granules of cloned NK and CTL (2, 3, 5). This view was supported by the demonstration that isolated granules from cloned CTL and from a NK-like tumor line mediated $Ca^{2+}$-dependent cytolysis, assemble poly-P1 and poly-P2 on target membranes, and cause $Ca^{2+}$-dependent conductance increase across planar bilayer membranes (4–8).

Isolated T-lymphocyte granules contain a number of protein bands identifiable by $NaDodSO_4$/polyacrylamide gel electrophoresis (for review, see ref. 9). Here, we report on the purification and functional characterization of the monomeric granule protein responsible for the formation of the 160-Å-wide polyperforin complex.

## MATERIALS AND METHODS

**Cells.** CTLL2 cells were grown in Iscove's modified Dulbecco's minimum essential medium (DMEM) as described (5). Five milliliters of packed cells was usually harvested from 6-liter cultures containing 10–15% rat spleen cell concanavalin A supernatant (5).

**Preparation of Granules.** Granules were prepared from 5 ml of packed CTLL2 cells that were washed in $Ca^{2+}$-free Hanks' balanced salt solution by Percoll density-gradient centrifugation as described (5). After fractionation of the Percoll gradients, granule-containing fractions, as identified by hemolytic assays (5), were pooled and used for the purification of P1.

**Purification of P1.** All reactions were carried out at 4°C unless stated otherwise. Granules isolated from Percoll gradients and containing Percoll were mixed with an equal volume of 1 M $NaKHPO_4$ buffer (pH 7.4) containing 10 mM benzamidine HCl, 1 mM EDTA, and 3 mM $NaN_3$. After addition of 2 mM phenylmethylsulfonyl fluoride, the mixture was allowed to stand on ice for 30 min. Addition of high phosphate concentrations to Percoll suspensions causes precipitation of Percoll as a white precipitate, which can be removed easily by centrifugation for 30 min at 20,000 rpm in the Sorvall centrifuge. The clear supernatant was harvested and the pellet was discarded. The supernatant was applied directly to a 2.5 × 90 cm column containing Sephacryl S-300 (Pharmacia) equilibrated with 0.1 M $NaKHPO_4$, pH 7.4/0.5 M NaCl/1 mM benzamidine HCl/1 mM EDTA/3 mM $NaN_3$. The sample was eluted at a flow rate of 25 ml/hr and 15-min fractions were collected. The fractions were assayed for protein and hemolytic activities. Hemolytically active fractions were pooled and dialyzed against 10 mM $NaKHPO_4$ buffer, pH 7.4/1 mM EDTA/3 mM $NaN_3$.

The dialyzed pool was applied to the Mono Q column of the fast protein liquid chromatography system by using the 50-ml superloop (Pharmacia). The superloop and the Mono Q column were kept in ice. The flow rate was 1 ml/min and, after sample application, the chromatogram was developed with an automatic gradient programer by using buffers A (10 mM $NaKHPO_4$, pH 7.4/1 mM EDTA/3 mM $NaN_3$) and B (same as buffer A with 2 M NaCl) and the following parameters: equilibration done with buffer A; after sample application, column washing with buffer A for 5 min; linear gradient for 35 min to final 50% A:50% B, followed by buffer B for 5 min. The column effluent was monitored by a flow cell at 280 nm and collected in 1-ml fractions on ice. The hemolytic activity of each fraction was determined.

**Hemolytic Assay for P1.** Sheep erythrocytes, washed and resuspended to 2–4 × $10^9$ per ml in 0.1-ml aliquots with 0.15 M NaCl/10 mM Tris·HCl, pH 7.2 (Tris/NaCl buffer), containing 5 mM $CaCl_2$, were incubated with 2- to 20-μl column fractions for 20 min at 37°C. Lysis was determined by dilution of samples to 2 ml with Tris/NaCl, followed by centrifugation and spectrophotometric quantitation of hemoglobin release

The publication costs of this article were defrayed in part by page charge payment. This article must therefore be hereby marked "*advertisement*" in accordance with 18 U.S.C. §1734 solely to indicate this fact.

Abbreviations: $\Delta\Psi$, membrane potential(s); P1, perforin 1; $Ph_4P^+$, tetraphenylphosphonium$^+$; NK, natural killer; CTL, cytoxic T lymphocyte(s).

in the supernatant at 541 nm. Z units of hemolysis are defined as in ref. 5.

**Metal Dependence of P1.** Sheep erythrocytes were washed in Tris/NaCl, to which $CaCl_2$ was added to the desired concentration. P1 was then added to the cell suspension, followed by incubation as above. Inhibition by $ZnCl_2$ was determined in the presence of 0.5 mM $CaCl_2$ in a similar manner.

**Membrane Potential ($\Delta\Psi$) Measurements.** The $\Delta\Psi$ of J774 macrophages was assayed by the uptake of [$^3$H]tetraphenylphosphonium ion ([$^3$H]$Ph_4P^+$) as described (10–12), with the following modifications. Cells were plated overnight on coverslips ($4 \times 10^4$ per ml, 1 ml per coverslip) in culture medium (DMEM/5% fetal bovine serum) prior to washing three times with low-$K^+$ buffer (118 mM NaCl/5 mM KCl/1.3 mM $CaCl_2$/0.8 mM $MgSO_4$/5.5 mM glucose/20 mM Hepes/9 mM $Na_2CO_3$, pH 7.4) and incubation with 20 $\mu$M [$^3$H]$Ph_4P^+$ for 30 min at 37°C. P1 was then incubated with the cells at 37°C for the indicated periods, at which time the medium was aspirated and coverslips were washed rapidly by dipping four times into separate beakers containing ice-cold phosphate-buffered saline ($P_i$/NaCl) and 1 mg of bovine serum albumin per ml. Cells were then lysed in 0.5 ml of 0.05% Triton X-100 in $H_2O$ and 0.25-ml aliquots were used for radioactivity determinations (12). The values of [$^3$H]$Ph_4P^+$ accumulated in the cells bathed in high-$K^+$ buffer (as in refs. 10–12) were used as background and were subtracted from values obtained with cells bathed in low-$K^+$ buffer. Conversion of corrected radioactivity into intracellular probe concentrations and $\Delta\Psi$ was done as described (10–12). Experiments with P1 were done in duplicate.

**Formation of Lipid Vesicles and Ion-Flow Measurements.** A mixture of phosphatidylethanolamine/phosphatidylcholine/cholesterol at 3:2:1 (wt/wt), 25 mM $\beta$-D-octyl glucoside in Hepes buffer (10 mM, pH 7.0, adjusted with Tris base) containing 0.05 M sodium isethionate, and 0.165 M sucrose (buffer C) was sonicated to clarity. Vesicles were formed by a one-step dilution with buffer C (1:100). Vesicles formed this way were collected by centrifugation at 100,000 $\times$ *g* for 90 min and resuspended to 10 mg/ml. The uptake of [$^3$H]$Ph_4P^+$ into lipid vesicles was quantitated by filtration (13). Briefly, the reaction was initiated by diluting 0.1 ml of lipid vesicles into 0.9 ml of buffer D (0.25 M sucrose/10 mM Hepes, pH 7.0) containing 50 $\mu$M [$^3$H]$Ph_4P^+$ with P1 (700 ng/ml) or control column buffer. At intervals, aliquots of the reaction mixture were filtered and washed, and radioactivity remaining on the filter was determined (13).

**Patch-Clamp Recording.** S49.1 T cells, maintained in culture as described (14), were washed and resuspended into low-$K^+$ buffer, with or without $Ca^{2+}$. Whole-cell recordings from these cells were obtained essentially as described (15). The cell dish was placed on the stage of a Nomarski optics microscope. Pipettes were fire-polished and used when resistance values ranged between 2 and 6 M$\Omega$. The pipette solution consisted of high-$K^+$ buffer, without $MgSO_4$ and containing 1.3 mM EGTA. High-resistance seals (>20 G$\Omega$) formed spontaneously on touching the cell surface with the pipette; whole-cell recording was obtained by application of strong negative pressure through the pipette. Currents were low-pass-filtered at 2 kHz and recorded on floppy disks in a 4094-2 Nicolet digital oscilloscope at sampling rates of 0.1–2 ms per point and simultaneously registered on a Gould 2200 S dual-pen recorder. Data were analyzed directly by using a software package available from Nicolet or transferred to a IBM PC for further analysis. Reagents were introduced into the cell medium by means of another micropipette (tip diameter, 4 $\mu$m) fitted onto a syringe, at 100 $\mu$m from cell.

**Other Assays.** Protein determination (16), NaDodSO$_4$/polyacrylamide gel electrophoresis (17), and electron microscopy were done as described (2).

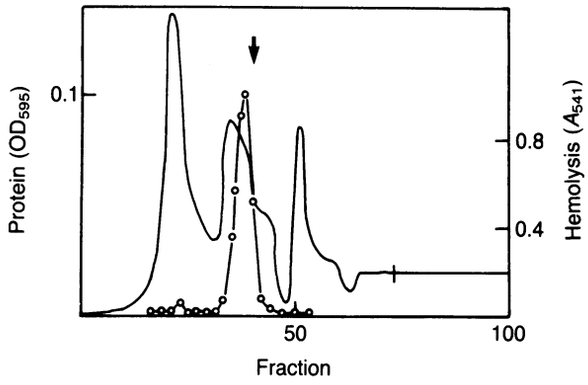


FIG. 1. Gel filtration of phosphate extract of granules. ○, Hemolytic activity; —, protein. The position of albumin marker is indicated by an arrow.

## RESULTS

**Purification of P1.** Solubilization of the cytolytic activity from isolated CTLL2 granules was effected by 0.5 M phosphate at pH 7.4 in the presence of protease inhibitors. This procedure was more effective than extractions with NaCl, KCl, or guanidine HCl (not shown). High phosphate, in addition, caused precipitation of Percoll, allowing its removal by centrifugation at 20,000 rpm. The soluble supernatant containing the cytolytic activity was then fractionated by gel filtration on Sephacryl S-300 (Fig. 1). Three major protein peaks eluted from the gel filtration column. Cytolytic activity was found in the trailing end of the center peak, eluting with an apparent molecular mass of 70–80 kDa. The active fractions were combined and, after dialysis, subjected to ion-exchange chromatography on Mono Q by using the fast protein liquid chromatography system. Fig. 2 shows the elution profile of protein and hemolytic activity from this column. Activity elutes in a single symmetrical peak containing only trace amounts of protein. Analysis of the pooled material by NaDodSO$_4$/polyacrylamide slab gel electrophoresis is shown in the Fig. 2 *Inset* in comparison to marker proteins. The active fractions contain a single protein band migrating with an apparent molecular mass of 75 kDa under reducing conditions (Fig. 2 *Inset*) and 58 kDA under nonreducing conditions (not shown). The mobility of this protein on NaDodSO$_4$ gels corresponds to the K1 band of isolated granules (5).

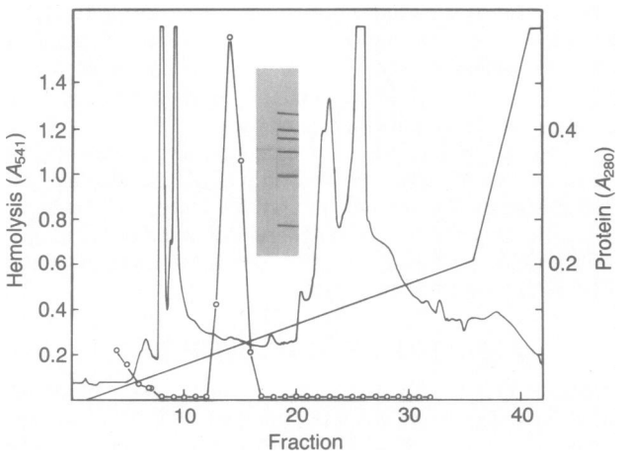


FIG. 2. Anion-exchange chromatography of pool from gel filtration. The fast liquid protein chromatography system and a Mono Q column were used. ○, Hemolytic activity; —, protein. The gradient ranges from 0 to 2 M NaCl.

Table 1. Purification of P1

| Fraction | Volume, ml | Protein, mg | Specific activity, Z/mg | Purification, fold |
|---|---|---|---|---|
| Granules | 15 | 45 | 80 | 1 |
| Perforin | 4 | 0.16 | 2187 | 27.3 |

Z units are as defined in ref. 5.

Table 1 shows the comparison of the hemolytic activity of granules with that of the isolated protein. The specific activity increased 27-fold during the purification procedure, with the recovery of 160 μg of apparently homogeneous protein from 45 mg of isolated granules.

**Hemolysis Induced by Purified P1.** Hemolysis mediated by P1 shows a sigmoidal dose–response curve similar to that observed with intact granules (Fig. 3*A*). The nonlinear dose–response at low input of granules of perforin is consistent with the putative polymerization of P1 during the cytolytic reaction. P1 and granules are absolutely dependent on $Ca^{2+}$ ions for lytic activity (Fig. 3*B*). Both isolated P1 and granules are inhibited by micromolar concentrations of $Zn^{2+}$ (Fig. 4*A*) and by preincubation with $Ca^{2+}$ (Fig. 4*B*). P1, in contrast to granules, is labile to incubation at 37°C in the absence of bivalent metal ions.

**Formation of Structural Membrane Lesions by P1.** Isolation of erythrocyte membranes subsequent to lysis by P1 and analysis by negative staining electron microscopy is shown in Fig. 5. Membrane lesions of ≈160 Å in diameter (Fig. 5) are formed that show the typical morphology of poly-P1. In addition to fully assembled ring structures, incompletely assembled tubules appearing as unclosed rings are also found (Fig. 5). These structures are incompletely assembled polymers of P1, which are also detectable when intact cells or granules lyse target cells. No structures corresponding to poly-P2 were found when cells were lysed with purified P1, indicating that poly-P2 complexes are assembled from different precursor molecules.

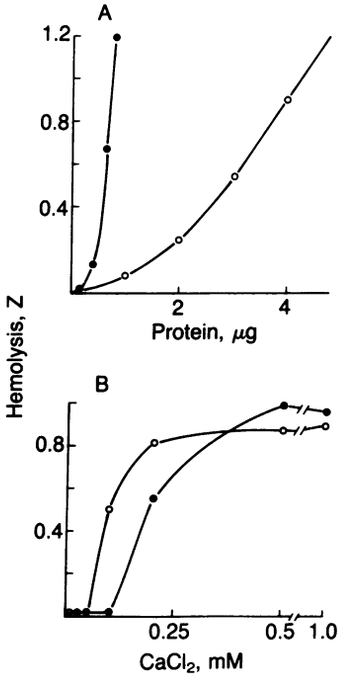


FIG. 3. (*A*) Dose–response of hemolysis mediated by isolated granules (○) and purified perforin (●). (*B*) Comparison of Ca dependence of lysis mediated by granules (○) and by P1 (●).

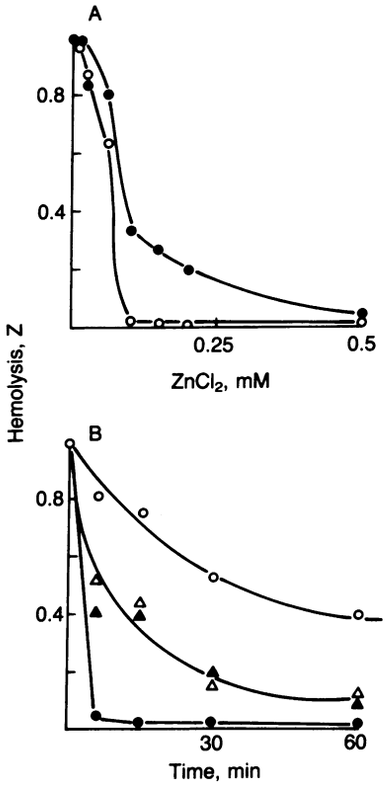


FIG. 4. (*A*) Inhibition of hemolysis by $ZnCl_2$ in the presence of 0.5 mM $CaCl_2$. ○, Granules; ●, P1. (*B*) Time-dependent loss of activity in the presence (filled symbols) and absence (open symbols) of 0.5 mM Ca at 37°C. Granules (○, ●) and P1 (△, ▲) were preincubated for the time indicated and the hemolytic activity was determined.

**Transmembrane Ion Flow Induced by Isolated P1.** The effects of P1 on the ΔΨ of J774 macrophages were assessed by the uptake of $[^3H]Ph_4P^+$ (10–12). The resting ΔΨ of plated macrophages averaged −70 mV, which was considerably higher than that obtained for cells in suspension (10–12). Exposure of cells to P1 in the presence of $Ca^{2+}$ resulted in a membrane depolarization, which showed only partial recovery after 45 min of incubation (Fig. 6). Membrane depolarization was not observed in $Ca^{2+}$-depleted medium but was induced with subsequent addition of 0.5 mM $Ca^{2+}$ (Fig. 6).

P1 also produced remarkable ion permeability changes in lipid vesicles (Fig. 7). An ion gradient was introduced across the membrane by diluting vesicles equilibrated with 50 mM

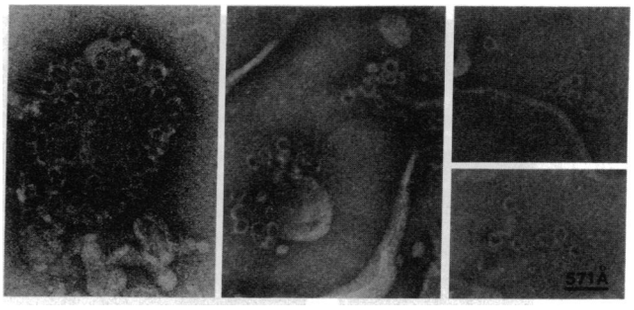

FIG. 5. Ultrastructural comparison of poly-P1 complexes assembled by intact CTLL2 (*Left*), by cytolytic granules isolated from CTLL2 (*Center*), and by purified P1 (*Right*) in the presence of $CaCl_2$. Lysed membranes were washed, incubated with L-1-tosylamido-2-phenylethyl chloromethyl ketone-treated trypsin (100 μg/ml) overnight at 22°C, washed again, and then mounted for electron microscopy by negative staining with uranyl formate (2%).

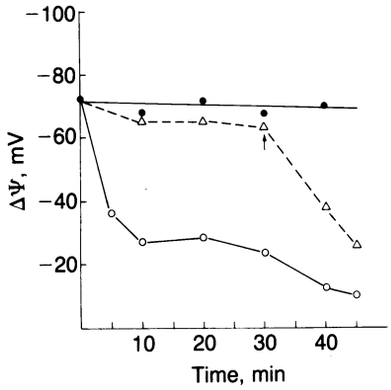


FIG. 6. Effect of P1 on J774 macrophage ΔΨ. J774 macrophages in low-$K^+$ buffer, loaded with $[^3H]Ph_4P^+$, were treated with 2 μg of P1 per ml at time 0 (○) or control Tris/NaCl buffer (●). P1 in Tris/NaCl was diluted 1:100 into cell medium. Cells washed and incubated in $Ca^{2+}$-free low-$K^+$ buffer (△) were treated with 2 μg of P1 per ml at time 0, followed by addition of $CaCl_2$ to a final concentration of 0.5 mM (arrow). Experiments carried out in duplicate at 37°C.

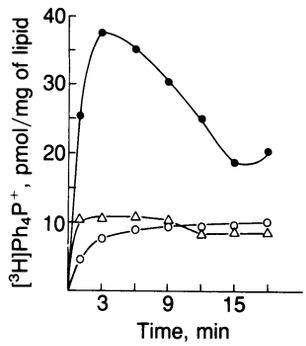


FIG. 7. Transmembrane ion flow in lipid vesicles induced by P1. Vesicles equilibrated with 50 mM sodium isothionate were diluted at time 0 into sucrose solution containing $[^3H]Ph_4P^+$ or P1 (1 μg/ml), with (●) or without (△) 1 mM $CaCl_2$. ○, Control vesicles diluted into sucrose solution, with $[^3H]Ph_4P^+$ and 1 mM $CaCl_2$. Data points represent the average of triplicate experiments performed at 37°C.

sodium isothionate into equiosmotic solutions of sucrose containing $[^3H]Ph_4P^+$. Since $Na^+$ ions permeate more rapidly through the poly-P1 channel than the larger anions (isothionate), a transient ΔΨ is produced by unequal accumulation of negative charges inside the vesicles in the presence of polymerizing P1 (Fig. 7). However, the vesicle ΔΨ was dissipated after a few minutes (Fig. 7), indicating that P1-treated vesicles were also made leaky to isothionate, albeit at a slower rate. Experiments with other electrolytes showed that in the presence of P1, lipid membranes became permeable to $Ca^{2+}$, $Mg^{2+}$, $EGTA^{2-}$, and $Tris^-$ (not shown). P1-treated-vesicles also became permeable to Lucifer yellow (molecular weight, 457) and sucrose (molecular weight, 342) (not shown). In all instances, the effect of P1 on transmembrane ion flow was absolutely $Ca^{2+}$-dependent (Fig. 7).

**Patch-Clamp Recording.** Whole-cell recording of S49.1 cells revealed resting ΔΨ of −55 ± 6 mV (31 cells), which were measured as the current-free steady-state potentials. Resting ΔΨ was largely dependent on the day of culture. Only cells at a density of $2 \times 10^4$ in culture were used for determination of resting ΔΨ. Very low leakage currents were observed at voltages around the resting potentials; the input resistance was often >10 GΩ. Following application of P1 (0.5 μg/ml), current increased in the inward direction, which occurred in a progressive manner, without any decay, resulting frequently in loss of the seal (Fig. 8*A*). The current increase could be dissociated as a summation of discrete current steps of 20–80 pA per unit (Fig. 8*B*), indicative of incorporation of single P1 channels into the cell membrane. The current effect produced by P1 was dependent on the presence of $Ca^{2+}$ (Fig. 8*C*). Single-channel recordings and kinetic analysis of channel openings were similarly obtained with membrane patches; results of these experiments will be described elsewhere. Single-channel fluctuations were rarely seen at resting potential levels (−55 mV); they became more frequent only at transmembrane potentials of >100 mV (not shown).

## DISCUSSION

This communication describes the isolation and characterization of a cytolytic protein from a murine, cytolytic T-lymphocyte clone. According to its putative function, this protein was named P1 (3) because it was thought to perforate membranes during polymerization on target cell surfaces. Evidence presented in Figs. 4 and 5 demonstrates that P1, in fact, produces structural and functional lesions consistent with this hypothesis. P1 is a 72- to 75-kDa protein that undergoes rapid $Ca^{2+}$-dependent polymerization and forms a tubular complex that functions as a large and voltage-independent transmembrane channel when inserted into membranes.

The activity of isolated P1 resembles closely the functional activity of cytolytic granules (see Figs. 3 and 4), including its ability to lyse a variety of tumor cells (not shown). An interesting difference is the lability of P1 at 37°C in the

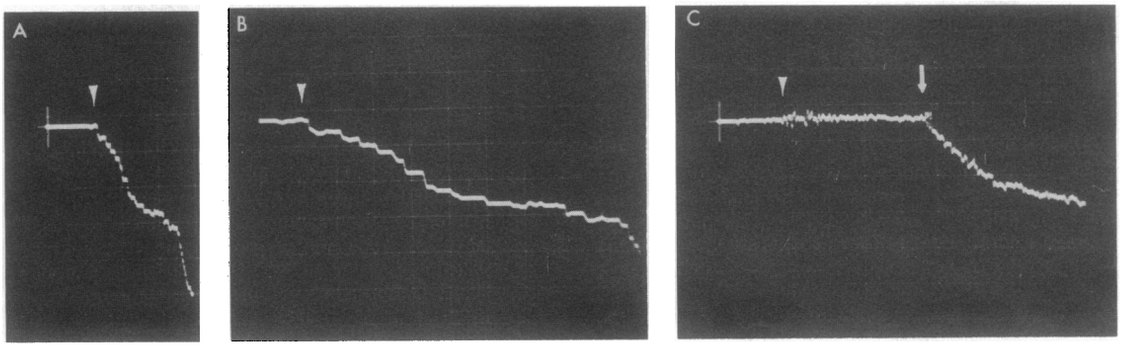


FIG. 8. Whole-cell currents recorded from S49.1 cells. Cells were clamped at −60 mV during P1 application. P1 (to 0.1 μg/ml) was added from a second micropipette at a distance of about 100 μm from the cell (arrowheads point to beginning of perfusion). (*A*) Cells bathed in low-$K^+$ buffer. (Scales per box: vertical, 200 pA; horizontal, 5 s.) (*B*) Horizontal expansion of *A*, 4×. (*C*) Cell bathed in $Ca^{2+}$-free low-$K^+$ buffer. Arrowhead points to addition of P1, as in *A*. $Ca^{2+}$ was added from a third pipette to a final concentration of 0.5 mM (arrow). Same scale as in *A*. Downward deflections represent inward currents.

absence of metal ions and the higher sensitivity of granules to $Ca^{2+}$ and $Zn^{2+}$. Possibly other granule proteins stabilize P1 and enhance the effect of metal ions inducing P1 polymerization.

Isolated P1 increases the ion permeability of bilayer membranes (Figs. 6–8). The increase in transmembrane ionic current represents the functional counterpart of structural membrane ring-like lesions by P1. As measured by whole-cell patch-clamp recordings, P1 induces voltage-insensitive ion channels on target membranes (Fig. 8). The functional activity of P1 on membranes depends absolutely on the presence of $Ca^{2+}$, an observation which provides further support for the $Ca^{2+}$-dependent polymerization of P1 to transmembrane ring-like tubular structures.

It is worthwhile to compare the structure and function of murine P1 to the human ninth component of complement (C9) (for review, see ref. 18). Both proteins polymerize to tubular complexes that cause membranolysis upon membrane insertion (19–21). C9 and P1 are inactivated by $Zn^{2+}$ ions at micromolar concentrations, a reaction that is accompanied by rapid polymerization of C9 (ref. 22; unpublished data). Whereas C9 polymerization under physiological conditions requires the assembly of the C5b-8 complex as C9 receptor (23, 24), P1 polymerization is not dependent on additional proteins and requires only low concentrations of $Ca^{2+}$ (Figs. 3 and 5). This difference is important because C5b-8 directs C9 polymerization to the target cell, thus preventing indiscriminate C9 polymerization. In the case of P1, directionality is achieved by compartmentalization of the cytolytic T cell and segregation of P1 in the granules, which, after specific target conjugation, are released onto the target membrane. Despite these differences, C9 and P1 show remarkable biochemical, structural, and functional homology, suggesting that they have arisen from an ancestral cytolytic protein and became specialized in humoral or cell-mediated cytolytic functions.

**Note Added in Proof.** While this work was in press, Masson and Tschopp (25) reported on purification of a similar pore-forming protein/P1 from cytolytic T-cell granules.

The excellent technical assistance of K. Penichet, R. Manganiello, S. S. Ko, and M. A. DiNome is heartily acknowledged. Discussions with A. Steinacker and A. Mauro on the patch-clamp system and C. F. Nathan were also most helpful. This work was supported by Public Health Service Grants CA39201 and AI21999 and American Cancer Society Grant IM396 to E.R.P., a fellowship from The Jane Coffin Childs Memorial Fund for Medical Research and a Cancer Research Institute grant to J.D.-EY., and Grants CA30198 and AI070127 from the National Institutes of Health to Z.A.C.

1. Dourmashkin, R. R., Deteix, P., Simone, C. B. & Henkart, P. A. (1980) *Clin. Exp. Immunol.* **42,** 554–560.
2. Podack, E. R. & Dennert, G. (1983) *Nature (London)* **302,** 442–445.
3. Dennert, G. & Podack, E. R. (1983) *J. Exp. Med.* **157,** 1483–1495.
4. Millard, P. J., Henkart, M. P., Reynolds, C. W. & Henkart, P. A. (1984) *J. Immunol.* **132,** 3197–3204.
5. Podack, E. R. & Konigsberg, P. J. (1984) *J. Exp. Med.* **160,** 695–710.
6. Young, J. D.-E, Nathan, C. F., Podack, E. R., Palladino, M. A. & Cohn, Z. A. (1985) *Proc. Natl. Acad. Sci. USA* **82,** in press.
7. Blumenthal, R., Millard, P. J., Henkart, M. P., Reynolds, C. W. & Henkart, P. A. (1984) *Proc. Natl. Acad. Sci. USA* **81,** 5551–5555.
8. Henkart, P. A., Millard, P. J., Reynolds, C. W. & Henkart, M. P. (1984) *J. Exp. Med.* **160,** 75–93.
9. Podack, E. R. (1985) *Immunol. Today* **6,** 21–27.
10. Young, J. D.-E, Young, T. M., Lu, L. P., Unkeless, J. C. & Cohn, Z. A. (1982) *J. Exp. Med.* **156,** 1677–1690.
11. Young, J. D.-E, Unkeless, J. C., Kaback, H. R. & Cohn, Z. A. (1983) *Proc. Natl. Acad. Sci. USA* **80,** 1636–1640.
12. Sung, S.-S. J., Young, J. D.-E, Origlio, A. M., Heiple, J. M., Kaback, H. R. & Silverstein, S. C. (1985) *J. Biol. Chem.*, in press.
13. Young, J. D.-E, Black, M., Mauro, A. & Cohn, Z. A. (1983) *Proc. Natl. Acad. Sci. USA* **80,** 3831–3835.
14. Mellman, I. S. & Unkeless, J. C. (1980) *J. Exp. Med.* **152,** 1048–1069.
15. Hamill, O. P., Marty, A., Neher, E., Sakmann, B. & Sigworth, F. J. (1981) *Pflugers Arch.* **391,** 85–100.
16. Bradford, M. (1976) *Anal. Biochem.* **72,** 248–254.
17. Laemmli, U. K. (1970) *Nature (London)* **227,** 680–685.
18. Podack, E. R. & Tschopp, J. (1984) *Mol. Immunol.* **21,** 589–603.
19. Podack, E. R. & Tschopp, J. (1982) *Proc. Natl. Acad. Sci. USA* **79,** 574–578.
20. Tschopp, J., Muller-Eberhard, H. J. & Podack, E. R. (1982) *Nature (London)* **298,** 534–538.
21. Young, J. D.-E, Cohn, Z. A. & Podack, E. R. (1985) *J. Cell. Biochem.*, in press.
22. Tschopp, J. (1984) *J. Biol. Chem.* **259,** 10569–10573.
23. Podack, E. R., Tschopp, J. & Muller-Eberhard, H. J. (1982) *J. Exp. Med.* **156,** 268–282.
24. Tschopp, J., Podack, E. R. & Muller-Eberhard, H. J. (1985) *J. Immunol.* **134,** 495–505.
25. Masson, D. & Tschopp, J. (1985) *J. Biol. Chem.* **260,** 9069–9072.